Yeast Miro GTPase, Gem1p, regulates mitochondrial morphology via a novel pathway

Rebecca L. Frederick,[1,2] J. Michael McCaffery,[3] Kyle W. Cunningham,[4] Koji Okamoto,[1,2] and Janet M. Shaw[1,2]

[1]Department of Biology and [2]Department of Biochemistry, University of Utah, Salt Lake City, UT 84112
[3]Integrated Imaging Center, Department of Biology, and [4]Department of Biology, Johns Hopkins University, Baltimore, MD 21218

Cell signaling events elicit changes in mitochondrial shape and activity. However, few mitochondrial proteins that interact with signaling pathways have been identified. Candidates include the conserved mitochondrial Rho (Miro) family of proteins, which contain two GTPase domains flanking a pair of calcium-binding EF-hand motifs. We show that Gem1p (yeast Miro; encoded by YAL048C) is a tail-anchored outer mitochondrial membrane protein. Cells lacking Gem1p contain collapsed, globular, or grape-like mitochondria. We demonstrate that Gem1p is not an essential component of characterized pathways that regulate mitochondrial dynamics. Genetic studies indicate both GTPase domains and EF-hand motifs, which are exposed to the cytoplasm, are required for Gem1p function. Although overexpression of a mutant human Miro protein caused increased apoptotic activity in cultured cells (Fransson et al., 2003. *J. Biol. Chem.* 278:6495–6502), Gem1p is not required for pheromone-induced yeast cell death. Thus, Gem1p defines a novel mitochondrial morphology pathway which may integrate cell signaling events with mitochondrial dynamics.

Introduction

Mitochondria are essential organelles whose morphology and activity adapt to physiological stresses and the changing metabolic state of the cell. Balanced mitochondrial division and fusion events help determine mitochondrial morphology in most organisms, and conserved proteins that mediate these processes have been identified (Hermann and Shaw, 1998; Yaffe, 1999; Jensen et al., 2000; Yoon and McNiven, 2001; Shaw and Nunnari, 2002; Westermann, 2002; Mozdy and Shaw, 2003; Osteryoung and Nunnari, 2003; Scott et al., 2003; Westermann, 2003; Chen and Chan, 2004). Much less is known about pathways that facilitate communication between mitochondria and other cellular compartments. Such pathways must exist, because mitochondrial division and cytochrome *c* release are essential for caspase-dependent apoptosis (Frank et al., 2001), mitochondria buffer cytosolic calcium levels (Brini and Carafoli, 2000; Sayer, 2002; Rizzuto et al., 2003; Jacobson and Duchen, 2004), and mitochondrial mass increases in response to cell growth. However, few mitochondrial proteins that interface with these pathways have been characterized.

The conserved mitochondrial Rho (Miro) family of proteins has the potential to coordinate cellular responses with mitochondrial dynamics and function. Miro proteins contain two GTPase domains, a pair of calcium binding EF-hand motifs (Fransson et al., 2003), and a COOH-terminal transmembrane domain (Wolff et al., 1999). The two Miro family members in mammalian cells, Miro-1 and Miro-2, localized to mitochondria in indirect immunofluorescence experiments (Fransson et al., 2003). Overexpression of Miro-1 containing a putative GTPase I activating mutation caused mitochondrial aggregation and increased apoptotic index (Fransson et al., 2003). These observations suggest that Miro proteins facilitate apoptosis and/or regulate mitochondrial dynamics.

Models for Miro function must take into account the behavior of cells lacking Miro protein, the importance of conserved functional domains, and the submitochondrial localization and topology of Miro proteins. For example, functional EF-hand motifs exposed to the cytoplasm would be in a position to sense changing cytosolic calcium levels, whereas localization of these motifs to the mitochondrial matrix could allow Miro to monitor organellar calcium. To address these issues and learn more about the cellular role of Miro, we analyzed the function of the single Miro homologue, Gem1p, in *S. cerevisiae*. Our studies demonstrate that Gem1p is a tail-anchored outer mitochondrial membrane protein required for normal mitochondrial dynamics. In addition, both GTPase domains and EF-hand

The online version of this article contains supplemental material.

Correspondence to Janet M. Shaw: shaw@bioscience.utah.edu; or Koji Okamoto: kokamoto@biology.utah.edu

Abbreviations used in this paper: 3-PGK, protein 3-phosphoglycerate kinase; Miro, mitochondrial Rho; MITO, mitochondrial pellet; mito-GFP, mitochondrial-targeted GFP; PK, proteinase K; PMS, post-mitochondrial supernatant; TEM, transmission electron microscopy; WCE, whole cell extract.

The Journal of Cell Biology, Vol. 167, No. 1, October 11, 2004 87–98
http://www.jcb.org/cgi/doi/10.1083/jcb.200405100

motifs, which are exposed to the cytoplasm, are required for function. Based on our findings, we suggest that Gem1p defines a novel pathway controlling mitochondrial dynamics.

Results

Yeast Miro (Gem1p) belongs to a novel gene family with predicted GTPases domains, EF-hand motifs, and a COOH-terminal transmembrane domain

The single Miro protein in *S. cerevisiae*, encoded by YAL048C, shares 30% identity and 48% similarity with the human Miro-1 protein. *GEM1* (for GTPase EF-hand protein of mitochondria) encodes a 662–amino acid protein with predicted molecular mass of 75.2 kD (Fig. 1 A). The GTPase I domain contains G1, G2, G4, and G5 motifs characteristic of Ras and Rho-like proteins, but lacks an apparent consensus G3 motif and the Rho-specific sequence insert (Bourne et al., 1991; Wennerberg and Der, 2004). The GTPase II domain is not closely related to Ras, Rho, or other GTPase families, but contains recognizable G1, G2, G4, and G5 motifs (unpublished data).

Gem1p contains a pair of CaM-like EF-hand motifs, each consisting of two α-helices that flank a 12 residue loop (Nakayama and Kretsinger, 1994; Ikura, 1996; Lewit-Bentley and Rety, 2000). In CaM-like EF-hand proteins, carboxylate side chains in positions 1, 3, 5, 9, and 12 of the loop act as electron donors for calcium coordination (Lewit-Bentley and Rety, 2000). This differs from a second class of EF-hand motifs (e.g., the first motif in the protein S100A), where calcium is coordinated via backbone oxygen atoms (Fig. 1 C).

Tail-anchored outer mitochondrial membrane proteins contain positively charged residues flanking a hydrophobic transmembrane sequence (Wattenberg and Lithgow, 2001; Borgese et al., 2003). Although our sequence alignments indicate that this targeting motif is also present in hMiro-1 (Fig. 1 D) and Gem1p (Wolff et al., 1999), the possibility that Miro family members are embedded in the outer mitochondrial membrane has not been tested. As in other known tail-anchored mitochondrial proteins like Fis1p (Wattenberg and Lithgow, 2001; Habib et al., 2003; Horie et al., 2003), hMiro-1 and Gem1p contain several positively charged residues adjacent to the transmembrane domain (Fig. 1 D, bold). These combined structural features suggest that Gem1p has calcium binding and GTPase activities and is tail-anchored in the outer mitochondrial membrane.

Cells lacking Gem1p respire poorly on synthetic glycerol medium

To determine whether Gem1p is required during mitotic growth, we replaced the entire *GEM1* ORF with a *HIS3* cassette in the W303 strain background. This *gem1*Δ strain was viable, but grew at a slightly reduced rate relative to wild type on solid medium containing dextrose (Fig. 2 A, SDextrose 30°C). The *gem1*Δ strain grew significantly slower than wild type on minimal media containing the nonfermentable carbon source glycerol (Fig. 2 A, SGlycerol 30°C). This defect was enhanced when the strain was grown at 37°C (Fig. 2 A). Introduction of a plasmid encoding wild-type Gem1p restored wild-type growth in *gem1*Δ cells (Fig. 2 A). Interestingly, DAPI staining indicated that mtDNA nucleoids were retained in ~75% of *gem1*Δ cells cultured in dextrose-containing medium overnight. Even after extended log-phase growth in dextrose-containing medium, 43% of *gem1*Δ cells retain detectable mtDNA (Fig. S1, available at http://www.jcb.org/cgi/content/full/jcb.200405100/DC1). These findings suggest that loss of Gem1p may cause secondary defects in mtDNA expression or integrity.

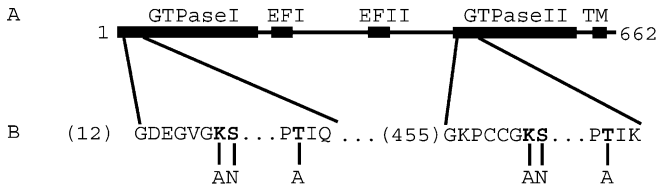

C Consensus EF hand:

				helix	loop	helix	
					1 3 5 9 12		
Gem1p	EFI	205	ALKRIFLLS	DL**N**QD**S**--YL**D**DN**E**	ILGLQKKC	233
Gem1p	EFII	334	FLVDIFLKF	DI**D**ND**G**--GL**N**NQ**E**	LHRLFKCT	362
hMiro-1	EFI	188	ALTRIFKIS	DQ**D**ND**G**--TL**N**DA**E**	LNFFQRIC	216
hMiro-1	EFII	308	FLQSTFDKH	DL**D**RD**C**--AL**S**PD**E**	LKDLFKVF	336
Cmd1p	EFI	12	EFKEAFALF	DK**D**NN**G**--SL**S**SS**E**	LATVMRSL	40
Cmd1p	EFII	48	EVNDLMNEI	DV**D**GN**H**--QL**E**FS**E**	FLALMSRQ	76
hS100A	EFI	11	TLINVFHAH	SGKEGDKYKL**S**KK**E**	LKELLQTE	40

D

Gem1p	623	TAA**K**DVDY**R**Q	*TALIFGSTVGFVALCSFTLM*	**K**LF**K**SS**K**FS**K** 662
hMiro-1	582	VTQADP**K**SST	*FWLRASFGATVFAVLGFAMY*	**K**ALL**K**Q**R** 618
Fis1p	121	ED**K**IQ**K**ETL**K**	*GVVVAGGVLAGAVAVASFFL*	RN**K**RR 155

Figure 1. **Domain structure of yeast Miro (Gem1p).** (A) Schematic representation of Gem1p domain structure. Indicated are the predicted GTPase I and II domains, EF-hand I and II motifs, and transmembrane segment (TM). (B) Vertical lines indicate substitutions generated in conserved residues of GTPase I and II domains (Table IV). (C) The consensus CaM (Cmd1p)-like EF-hand motif consists of a helix-loop-helix and is indicated (top). Residues important for calcium coordination are bold. Underlined E in Gem1p(EF I) and Gem1p(EF II) were converted to K for mutational analysis (Table IV). (D) Amino acids 633–652 in the Gem1p COOH terminus are predicted to form a membrane spanning α-helix (Wolff et al., 1999). A similar hydrophobic stretch is present in hMiro-1, other Miro homologues (not depicted), and Fis1p, a tail-anchored outer mitochondrial membrane protein. Predicted transmembrane segments are in italics. Positively charged residues predicted to contribute to mitochondrial membrane targeting are indicated in bold.

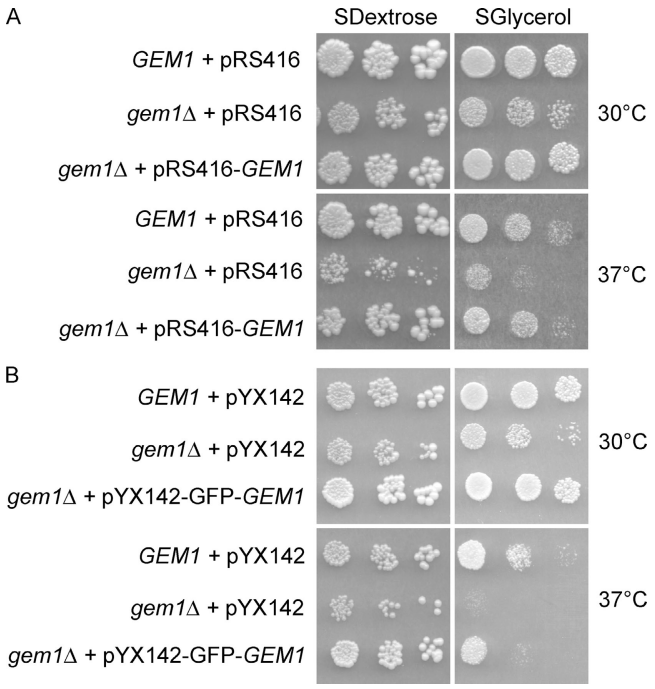

Figure 2. **Cells lacking Gem1p grow slowly on synthetic glycerol medium.** Strains (JSY7000 *GEM1* or JSY7002 *gem1*Δ) with the indicated plasmid were spotted on SDextrose or SGlycerol lacking the appropriate amino acid and grown for 3 d at the indicated temperature. (A) Gem1p expressed from its own promoter (pRS416-*GEM1*) complements the *gem1*Δ glycerol growth defect. (B) GFP-Gem1p expressed from the TPI promoter (pYX142-GFP-*GEM1*) partially complements the *gem1*Δ glycerol growth defect.

*gem1*Δ cells have distorted mitochondrial morphology but maintain inner membrane cristae structures

In wild-type yeast, mitochondria form a branched tubular network located at the cell cortex (Stevens, 1981; Koning et al., 1993). When visualized with a mitochondrial-targeted GFP (mito-GFP), 86.6% of cells in a wild-type population displayed a tubular mitochondrial network (Fig. 3 A). In contrast, cells lacking Gem1p had pronounced defects in mitochondrial distribution and morphology. As shown in Fig. 3 C, 53.7% of *gem1*Δ cells contained mitochondria that were globular with an irregular perimeter. Aberrant mitochondria of this type were never observed in wild-type strains ($n > 1000$). These large mitochondria did not appear to be collapsed tubules, as labeling with an outer membrane targeted form of GFP resulted in rim staining that enclosed matrix-targeted RFP (unpublished data). Other mitochondrial morphologies, including grape-like clusters (24%; Fig. 3 D) and collapsed mitochondria (16%; Fig. 3 B) were also observed in *gem1*Δ cells. The grape-like mitochondrial clusters were larger and fewer in number than mitochondrial fragments observed in a mitochondrial fusion mutant (*fzo1*Δ; Fig. 3 E). Collapsed mitochondria (Fig. 3 B) were frequently thicker than wild-type mitochondrial tubules and had variations in diameter along the length of the tubule. Because these collapsed mitochondria retain their tubular structure, they were not included in the "mutant" category during phenotypic quantification. Globular (Fig. 3 C), grape-like (Fig. 3 D), and fragmented (Fig. 3 E) mitochondria were scored in a single category, designated "Percent mutant" (Table I), unless otherwise indicated. A plasmid containing *GEM1* expressed from its own promoter restored tubular networks in 69.3% of the *gem1*Δ population (Table I). In the FY strain background, deletion of *gem1* had a less severe affect on mitochondrial morphology (unpublished data). Overexpression of full-length Gem1p or Gem1p(1-632) lacking the putative transmembrane domain from a galactose-inducible promoter did not cause defects in mitochondrial morphology in wild-type cells (unpublished data).

To determine whether inner mitochondrial membrane ultrastructure was disrupted in *gem1*Δ cells, we performed transmission electron microscopy (TEM). Both wild-type and *gem1*Δ sections contained mitochondrial profiles with well-developed inner membrane cristae (Fig. 4). In wild-type cells, mitochondria in longitudinal sections appeared tubular (Fig. 4 A) and in cross section (Fig. 4 B) were surrounded by a double membrane. *gem1*Δ sections often exhibited large mitochondrial profiles with double membranes and lighter matrix staining, consistent with the idea that these organelles are swollen (Fig.

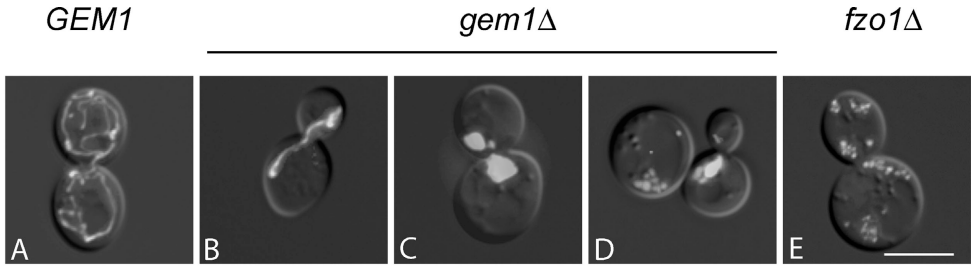

Strain	% tubular network	% collapsed tubule	% globular	% grapes	% fragmented
GEM1	86.6 ± 2.6	6.7 ± 2.7	0 ± 0	4.9 ± 2.1	1.8 ± 1.5
*gem1*Δ	3.4 ± 1.1	16.1 ± 3.2	53.7 ± 1.7	24.1 ± 2.3	2.7 ± 1.7

Figure 3. **Mitochondrial morphology is abnormal in cells lacking Gem1p.** Mitochondrial morphologies are shown for *GEM1* cells (A), *gem1*Δ cells (B–D), and fusion-deficient *fzo1*Δ cells (E) expressing mito-GFP and grown in SDextrose medium at 30°C to mid-log phase (OD_{600} 0.5–1.5). GFP fluorescent and DIC images are superimposed for each cell. The percentage of cells in a *GEM1* or *gem1*Δ culture with the morphologies depicted in A–E is shown (bottom). $n = 900$. Bar, 5 μm.

Table I. **Mitochondrial morphology in *GEM1* and *gem1*Δ cells**

Genotype	Plasmid	Percent tubular network	Percent collapsed	Percent mutant
GEM1	None	86.6 ± 2.6	6.7 ± 2.7	6.7 ± 2.3
*gem1*Δ	None	3.4 ± 1.1	16.1 ± 3.2	80.5 ± 3.3
GEM1	pRS416	85.8 ± 1.8	7.4 ± 3.0	6.8 ± 1.9
*gem1*Δ	pRS416	2.2 ± 1.3	19.6 ± 6.2	78.2 ± 6.9
*gem1*Δ	pRS416-*GEM1*	69.3 ± 5.0	14.8 ± 4.6	15.8 ± 3.8
GEM1	pYX142	84.3 ± 1.5	9.0 ± 1.0	6.7 ± 1.2
*gem1*Δ	pYX142	0.9 ± 0.8	20.7 ± 5.3	78.5 ± 4.5
*gem1*Δ	pYX142-GFP-*GEM1*	57.9 ± 11.3	24.1 ± 11.6	18.0 ± 3.2

$n_{cells} \geq 500$.
Mitochondria were visualized by expressing mito-RFP or mito-GFP.
Percent tubular network contains wild-type morphology shown in Fig. 3 A.
Percent collapsed contains aberrant morphology shown in Fig. 3 B.
Percent mutant category contains aberrant morhpologies shown in Fig. 3 (C–E).

4, C–F). These findings provide additional evidence that globular mitochondria in *gem1*Δ cells are not composed of aggregated tubules. Interestingly, *gem1*Δ mitochondria in a few TEM sections appeared partially or completely engulfed by vacuoles, suggesting that aberrant mitochondria are turned over via autophagy (unpublished data).

Disruption of actin cytoskeleton or ER organization can cause secondary defects in mitochondrial morphology and inheritance (Drubin et al., 1993; Hermann et al., 1997; Prinz et al., 2000; Singer et al., 2000). However, mitochondrial morphology defects in *gem1*Δ cells are not due to disruption of these structures. Alexa-Phalloidin staining studies showed actin cytoskeletal organization was normal in 99.5% of *GEM1* and *gem1*Δ cells ($n = 200$). Moreover, actin-based transport of mitochondria remained intact as medium and large-budded *gem1*Δ cells always inherit mitochondria (Fig. 5). The lack of mitochondria observed in some small-budded *gem1*Δ cells is likely a delay in movement of large globular organelles to the bud. Vacuole inheritance, another actin-based process in yeast (Hill et al., 1996), was not disrupted in *gem1*Δ strains. In pulse-chase experiments, FM 4-64–labeled vacuoles were inherited by 98.3 and 95.8% of wild-type and *gem1*Δ buds, respectively ($n = 120$). In addition, yeast nuclei (visualized by DAPI staining) and ER morphology (visualized by expression of Sec63-GFP) were normal in the absence of Gem1p (unpublished data). Vacuolar morphology and endocytic function also appeared wild type when tested by monitoring internalization of the vital dye FM 4-64 (unpublished data). Together, these data suggest that disruption of *GEM1* causes primary defects in mitochondrial morphology and function but does not disturb organization of other cellular structures.

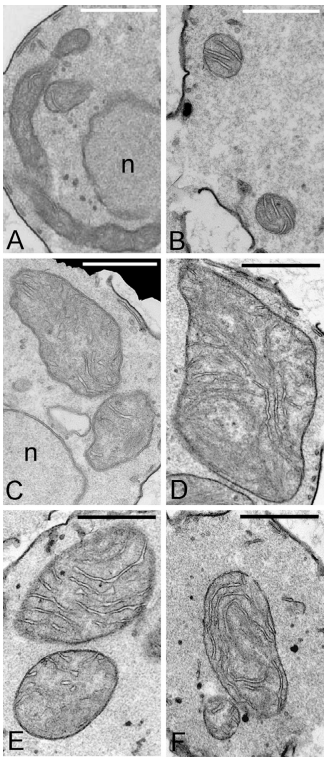

Figure 4. **Inner membrane cristae are present in globular *gem1*Δ mitochondria.** Mitochondria in wild-type cells (JSY7000) are tubular in longitudinal sections (A) and spherical in cross section (B) and contain inner membrane cristae. Profiles of globular mitochondria in *gem1*Δ strains (JSY7002, C–F), are larger than wild type but contain well-developed cristae. n, nucleus. Bars, 1 μm.

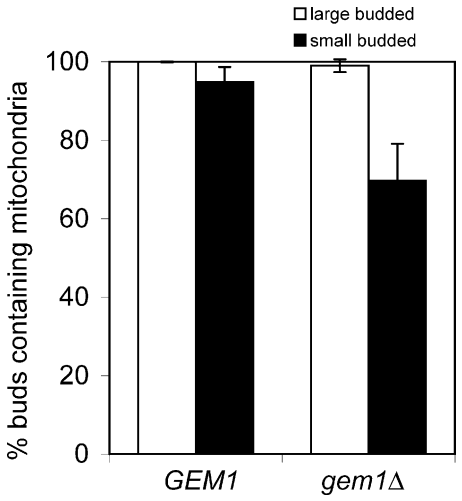

Figure 5. **Mitochondrial inheritance is not blocked in the absence of Gem1p.** mito-GFP-labeled mitochondria were observed in strains grown to mid-log phase. Large- or small-budded cells containing mitochondria in the bud were scored. $n > 250$.

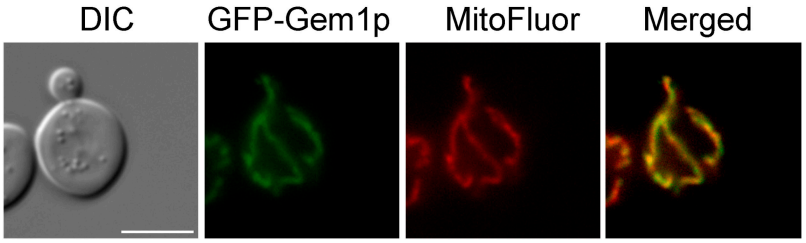

Figure 6. **GFP-Gem1p localizes to mitochondria.** Wild-type cells (JSY7000) with pYX142-GFP-*GEM1* were grown to late log phase (OD_{600} ~2) in SDextrose. Mitochondria were stained with MitoFluor red 589. Bar, 5 μm.

Gem1p is a tail-anchored outer membrane protein with its functional domains exposed to the cytoplasm

To determine where Gem1p localizes in vivo, we fused GFP to the NH_2 terminus of a constitutively expressed Gem1p (pYX142-GFP-*GEM1*). This construct complements the glycerol growth (Fig. 2 B) and mitochondrial morphology defects (Table I) of *gem1* null cells at 30°C. When expressed in wild-type cells, GFP-Gem1p uniformly labeled mitochondrial tubules that were costained with MitoFluor red 589 (Fig. 6).

Subcellular fractionation studies confirmed that Gem1p is a mitochondrial protein (Fig. 7 A). When whole cell extracts (WCEs) from wild-type cells expressing GFP-Gem1p were separated into post-mitochondrial supernatant (PMS) and mitochondrial pellet (MITO) fractions, GFP-Gem1p was found in the MITO, along with the integral outer mitochondrial membrane protein porin. In contrast, GFP-Gem1p was not detected in the PMS, which contained the cytoplasmic protein 3-phosphoglycerate kinase (3-PGK).

Protease protection assays indicated that GFP-Gem1p is an outer mitochondrial membrane protein (Fig. 7 B). When intact mitochondria were treated with proteinase K (PK), both Fzo1p (an outer membrane protein) and GFP-Gem1p were efficiently degraded. In contrast, the intermembrane space protein Cyb2p was protected from externally added PK, indicating that the outer membrane was not compromised. PK did degrade Cyb2p when mitochondria were subjected to osmotic shock, a treatment that causes mitochondria to swell, rupturing the outer membrane while leaving the inner membrane intact. When membranes were solubilized using Triton X-100 in the presence of PK, the matrix protein mtHsp70 was also degraded. Because the GFP tag is fused to the NH_2 terminus of the protein, these results demonstrate that Gem1p is localized to the outer mitochondrial membrane with its NH_2 terminus exposed to the cytoplasm.

Although the membrane association of Miro proteins has never been analyzed, several observations suggest that these GTPases are tail-anchored outer membrane proteins. First, like other mitochondrial outer membrane proteins, Miro family members do not contain a classical mitochondrial targeting signal. Second, previous studies showed that, like other tail-anchored proteins, COOH-terminal–tagged forms of Gem1p were not expressed (Wolff et al., 1999). Third, Miro family members, including Gem1p, contain a predicted COOH-terminal transmembrane domain (Fig. 1 D). To test whether Gem1p is an integral membrane protein, we performed carbonate extraction on isolated mitochondria. Upon sodium carbonate treatment under alkaline conditions, peripheral membrane proteins and soluble components can be released from mitochondria into the supernatant, whereas integral membrane proteins remain membrane associated. The mitochondrial membrane pel-

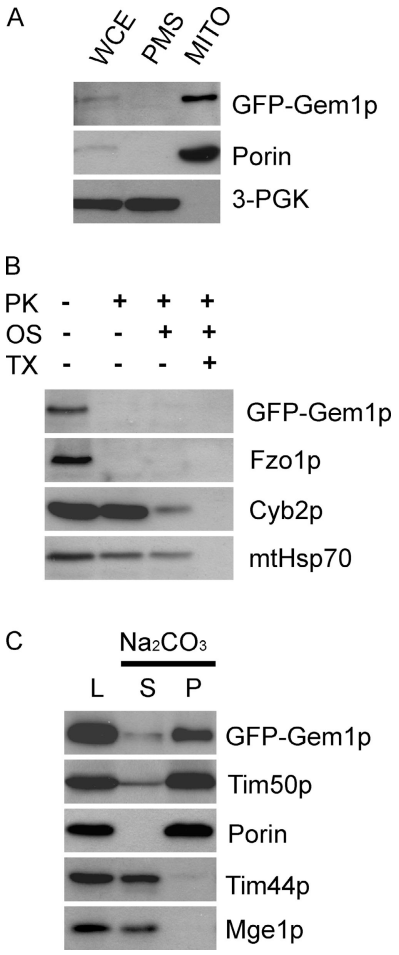

Figure 7. **Gem1p is a single-pass outer mitochondrial membrane protein with its NH_2 terminus exposed to the cytoplasm.** (A) WCE from JSY7000 (*GEM1*) expressing GFP-Gem1p was fractionated by differential centrifugation to yield PMS and MITO pellet, and analyzed by SDS-PAGE and Western blotting with antibodies against GFP, the multi-pass outer mitochondrial membrane protein Porin, and the cytoplasmic protein 3-PGK. WCE and PMS, 1× cell equivalents; MITO, 10× cell equivalents. (B) Untreated, osmotically shocked (OS), or Triton X-100 solubilized (TX) mitochondria were treated with (+) or without (−) PK and analyzed by SDS-PAGE and Western blotting with antibodies specific for GFP, the integral outer membrane protein Fzo1p, the intermembrane space protein Cyb2p, and the matrix protein mtHsp70. (C) Mitochondria (200 μg) were treated with sodium carbonate (pH 11.5) and separated into supernatant (S) and pellet (P) fractions. One-sixth of the reaction was loaded in each lane (L, load, untreated mitochondria). Tim50p is a single-pass inner membrane protein. Tim44p is a peripheral membrane protein in the matrix. Mge1p is a soluble matrix protein.

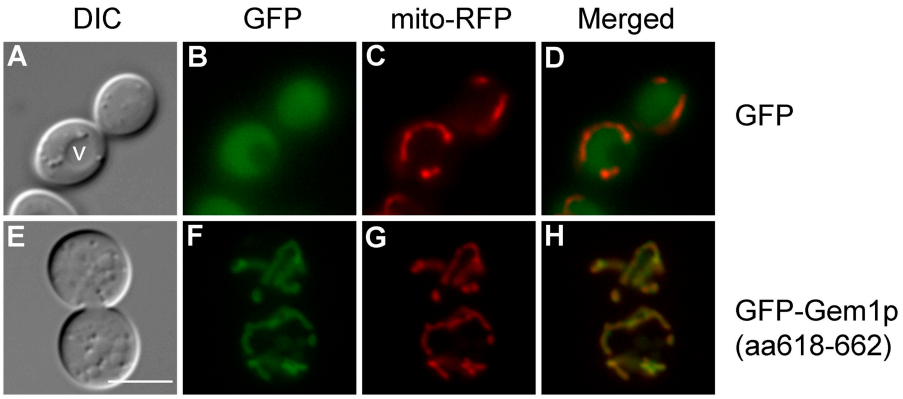

Figure 8. **The COOH-terminal 45 aa of Gem1p are sufficient for mitochondrial targeting.** Images of *GEM1* cells (JSY7000) expressing GFP alone (A–D) or GFP-Gem1p (aa618-662) (E–H) are shown. Mitochondria were visualized simultaneously with mito-RFP. v, vacuole. Bar, 5 μm.

let and supernatant were fractionated and analyzed for the presence of known membrane proteins and GFP-Gem1p (Fig. 7 C). Although GFP-Gem1p was partially extracted by carbonate treatment, most of the protein remained in the membrane fraction. Previous studies indicate that some single-pass transmembrane proteins can be partially extracted by carbonate treatment (Mokranjac et al., 2003; Truscott et al., 2003). Consistent with these findings, the single-pass transmembrane protein Tim50p was found in both the supernatant and pellet fractions. Porin, a multi-pass transmembrane protein, was present exclusively in the membrane pellet (Fig. 7 C). The peripheral membrane protein Tim44p and the soluble matrix protein Mge1p were detected only in the supernatant. Together with the protease protection results, these findings indicate that Gem1p is a single-pass outer mitochondrial membrane protein.

To confirm that Gem1p behaves like a tail-anchored protein, we verified that the COOH-terminal 45 aa of Gem1p were sufficient to localize GFP to mitochondria (Fig. 8, E–H). When GFP was fused to residues 618–662 of Gem1p, GFP-associated fluorescence completely overlapped with mito-RFP-labeled mitochondria. In a control experiment, GFP expressed in wild-type cells localized to the cytoplasm with visible exclusion from the vacuole (Fig. 8, A–D). GFP-Gem1p lacking amino acids 618–662 was found in the cytoplasm (unpublished data), indicating that the COOH terminus is required for targeting. Because amino acids 633–652 are hydrophobic and predicted to span the membrane as a single α-helix (Fig. 1 D), this topology would place the COOH-terminal 10 aa of Gem1p in the intermembrane space.

Gem1p is not required for mitochondrial division and fusion events

The yeast mitochondrial network is maintained by balanced division and fusion events. Mutations in genes required for fusion, including *FZO1* and *UGO1*, cause mitochondrial fragmentation due to unopposed division (Bleazard et al., 1999; Sesaki and Jensen, 1999, 2001). In contrast, mutations in genes required for mitochondrial division, like *DNM1,* result in net formation due to ongoing fusion (Bleazard et al., 1999; Sesaki and Jensen, 1999). Because Gem1p affects mitochondrial morphology, we asked whether Gem1p is required for Dnm1p-mediated mitochondrial division events or Fzo1p-mediated fusion events.

A yeast mating assay can be used to monitor mitochondrial fusion in vivo. After zygote formation, mitochondria from each haploid cell fuse, and their contents mix (Nunnari et al., 1997). When mitochondria from each haploid parent are labeled either with mito-RFP or mito-GFP, mixing of contents in fused mitochondria appears as complete overlap of red and green fluorescence. Previous studies showed that zygotes lacking the division gene *DNM1* (*dnm1*Δ) fuse as efficiently as wild type (Bleazard et al., 1999). However, zygotes lacking the fusion genes *UGO1* (*ugo1*Δ) (Sesaki and Jensen, 2001) or *FZO1* (Hermann et al., 1998) contain fragmented mitochondria that fail to fuse. Disruption of *DNM1* in *ugo1*Δ and *fzo1*Δ strains blocks fragmentation but does not restore fusion (Bleazard et al., 1999; Sesaki and Jensen, 2001).

As shown in Table II, mitochondrial fusion occurs at near wild-type levels (*GEM1 DNM1 UGO1*, 98.1%) in zygotes lacking Gem1p (*gem1*Δ *DNM1 UGO1*, 85.9%). Absence of Dnm1p did not dramatically change the efficiency of mitochondrial fusion (*gem1*Δ *dnm1*Δ *UGO1*, 80.9%). In contrast, mitochondrial fusion was completely blocked in zygotes lacking both Ugo1p and Dnm1p (*GEM1 dnm1*Δ *ugo1*Δ, 0.0%). The slightly reduced rate of mitochondrial fusion in the absence of Gem1p is likely due to morphology changes that prevent efficient mitochondrial collision in zygotes. Nevertheless, aberrant mitochondria in *gem1*Δ cells are clearly competent for fusion. Moreover, in *gem1*Δ *dnm1*Δ strains, some mitochondrial nets can be observed, indicating that mitochondrial fusion is occurring (unpublished data).

Table II. **Mitochondrial fusion in budded zygotes**

Strains mated	No. of fused mitochondria /total scored	Percent fusion observed
GEM1 DNM1 UGO1 × *GEM1 DNM1 UGO1*	157/160	98.1
*gem1*Δ *DNM1 UGO1* × *gem1*Δ *DNM1 UGO1*	177/206	85.9
*gem1*Δ *dnm1*Δ *UGO1* × *gem1*Δ *dnm1*Δ *UGO1*	131/162	80.9
*GEM1 dnm1*Δ *ugo1*Δ × *GEM1 dnm1*Δ *ugo1*Δ	0/157	0.0

Large-budded zygotes containing both mito-RFP and mito-GFP were scored at 2.5–4 h after mating on YPD.

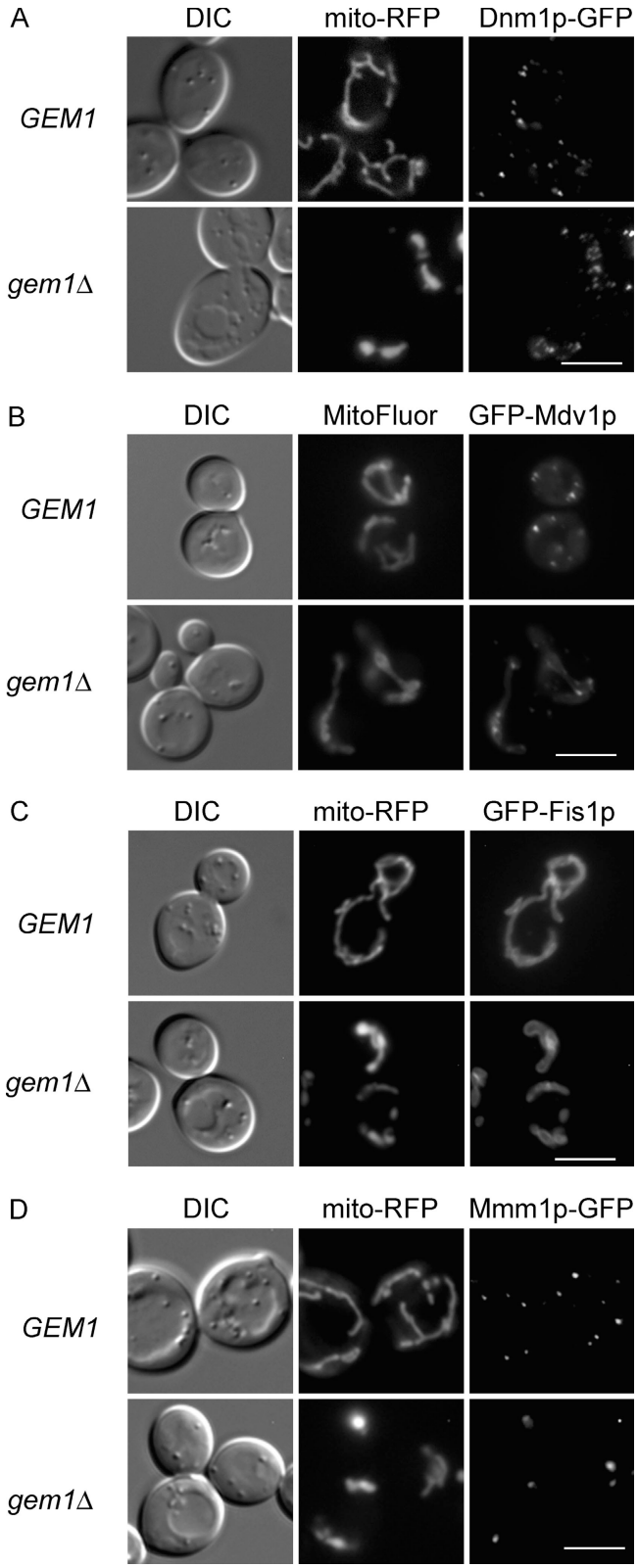

Figure 9. **Previously characterized mitochondrial morphology proteins are properly localized in *gem1*Δ cells.** Colocalization of mitochondria and GFP-labeled Dnm1p (A), Mdv1p (B), Fis1p (C), and Mmm1p (D) was observed in log phase *GEM1* and *gem1*Δ cells. Bars, 5 μm.

Mitochondrial fragmentation in an *fzo1* mutant requires active mitochondrial division. To test whether Gem1p is required for mitochondrial division, we asked if *gem1*Δ could prevent division and fragmentation in an *fzo1*Δ mutant strain. In both the *gem1*Δ *fzo1*Δ test strain and the *GEM1 fzo1*Δ control strain, mitochondria fragment in the majority of the population (91.1%, 99.0% respectively, Table III). Similar results were obtained when the temperature-sensitive *fzo1-1* allele was used for these studies (unpublished data). Moreover, in *gem1*Δ cells, components of the division machinery, including Dnm1p, Mdv1p, and Fis1p (Otsuga et al., 1998; Bleazard et al., 1999; Fekkes et al., 2000; Mozdy et al., 2000; Tieu and Nunnari, 2000; Cerveny et al., 2001) were properly localized as mitochondrial puncta (Dnm1p, Mdv1p; Fig. 9, A and B) or uniformly on the mitochondrial network (Fis1p; Fig. 9 C), supporting the notion that division is not impaired in this strain. Steady-state levels of Fis1p, Dnm1p, Mdv1p, and Fzo1p in *gem1*Δ cells were wild type (unpublished data), suggesting that Gem1p does not regulate stability of these mitochondrial morphology proteins.

Both GTPase domains I and II and the EF-hand motifs are required for Gem1p function

To determine whether the predicted functional domains of Gem1p were required for its role in maintenance of tubular mitochondrial morphology, we generated mutations in conserved residues of each GTPase domain (Fig. 1 B) or the EF-hand motifs (Fig. 1 C). Similar mutations in known GTPases and EF-hand motifs have been shown to abrogate function. Mutation of K16 in Ras disrupts GTP nucleotide binding (Sigal et al., 1986). Mutation of S17 in Ras reduces affinity for GTP by 20–40-fold (Feig and Cooper, 1988). Finally, mutation of the conserved threonine (T35) residue in Ras disrupts GTPase activating protein (GAP) binding such that GTP hydrolysis cannot be stimulated efficiently (Cales et al., 1988). In *GEM1*, none of these mutations caused dominant mitochondrial morphology defects in wild-type strains (unpublished data). GFP-tagged versions of all mutant Gem1 proteins were expressed and localized to mitochondria (unpublished data).

When *gem1*Δ cells contained a plasmid expressing full-length wild-type Gem1p, 59.9% of cells in a population had tubular mitochondrial networks, whereas only 14.6% contained mutant mitochondria (Table IV). Mutation of conserved residues in the nucleotide binding domain of GTPase I completely abrogated protein function. When K18 was mutated to alanine (K18A) in Gem1p, 75.8% of cells displayed mutant mitochondria, similar to *gem1*Δ cells containing the vector with no insert (83.3% mutant). Similarly, expression of Gem1p(S19N) did not rescue *gem1* null cells (79.1% mutant). Mutation in the effector binding domain of GTPase I did not prevent Gem1p function, as 57.8% of *gem1*Δ cells expressing Gem1p(T33A) contained tubular networks. Based on mutational analysis of known GTPases, these data suggest that the nucleotide binding activity of GTPase I domain is required for function. Whether this domain requires accessory proteins for nucleotide exchange or hydrolysis remains to be determined.

Table III. **Mitochondrial division and fragmentation occurs in *fzo1*Δ lacking Gem1p**

Genotype	Percent tubular network	Percent collapsed	Percent globular and large grapes	Percent fragmented
GEM1 FZO1	82.7 ± 5.7	8.0 ± 2.5	0.0 ± 0.0	9.3 ± 3.1
*gem1*Δ *FZO1*	0.0 ± 0.0	18.3 ± 6.6	68.5 ± 8.0	13.2 ± 5.3
*GEM1 fzo1*Δ	0.0 ± 0.0	1.0 ± 1.8	0.0 ± 0.0	99.0 ± 1.8
*gem1*Δ *fzo1*Δ	0.0 ± 0.0	3.2 ± 2.2	5.6 ± 6.3	91.1 ± 6.9

$n_{cells} > 300$.
Mitochondria were visualized by expressing mito-GFP.
Percent tubular network contains wild-type morphology shown in Fig. 3 A.
Percent collapsed contains aberrant morphology shown in Fig. 3 B.
Percent globular and large grapes contains aberrant morphologies shown in Fig. 3 (C and D).
Percent fragmented contains aberrant morphology shown in Fig. 3 E.

The GTPase II domain of Gem1p is also important for function (Table IV). Similar mutations of the conserved lysine and serine residues within the GTPase II P-loop and the conserved threonine in the effector binding domain were analyzed (Fig. 1 B). In *gem1*Δ strains expressing Gem1p(S462N), 80.3% of cells contained mutant mitochondria, similar to *gem1*Δ cells containing vector with no insert (83.3% mutant). When *gem1*Δ strains expressing Gem1p(K461A) or Gem1p(T480A) were scored, the percentage of cells with mutant mitochondria (55.3 and 48.3%, respectively) was somewhat lower than vector alone (83.3%), suggesting that these mutant proteins may have retained partial function. Because Gem1p(S462N) cannot rescue *gem1*Δ mutant mitochondria, these data demonstrate that the GTPase II domain is essential for Gem1p function.

Finally, we examined the role of the EF-hand motifs in Gem1p function. Calcium binding activity of EF-hand motifs in CaM can be abrogated by mutation of a conserved loop glutamine to lysine (Feng and Stemmer, 2001). We analyzed a mutant protein in which either residue E225 of EF I or residue E354 of EF II were replaced with a lysine (K) residue (Fig. 1 C). As some multiple EF-hand proteins require mutation of both EF-hand motifs to cause a marked decrease in protein function (Janssens et al., 2003), a protein containing both E225K and E354K mutations was also analyzed. As shown in Table IV, Gem1p containing only one EF-hand motif mutation had partial function (E225K 28.7% tubular, E354K 42.2% tubular). In contrast, the function of Gem1p(E225K,E354K) was dramatically impaired with only 14.3% of cells in a population displaying branched tubular mitochondria. Mutation of either or both of these conserved glutamine residues to alanine partially abrogated protein function similar to the lysine substitutions (unpublished data). These results establish that the EF-hand motifs are important for Gem1p function.

Gem1p is not required for cell death induced by α-factor mating pheromone

Overexpression of a putative hyperactive Miro-1 variant in COS-7 cells results in a high rate of spontaneous apoptosis (Fransson et al., 2003). Previous studies in yeast demonstrated that apoptosis-like cell death occurs after prolonged treatments with α-factor, a pheromone that induces mating and calcium signaling pathways that help to prevent cell death (Iida et al., 1990; Cyert et al., 1991; Cyert and Thorner, 1992; Foor et al., 1992; Moser et al., 1996; Withee et al., 1997; Muller et al., 2001; Severin and Hyman, 2002). To test whether Gem1p might perform a similar "pro-death" function in yeast, we measured the degree of cell death in wild-type and *gem1* mutant cultures after a 10-h treatment with α-factor in the presence and absence of FK506, an inhibitor of calcineurin in the calcium signaling pathway. The levels of cell death in *gem1* cultures were indistinguishable from those of wild-type cultures at all incubation times (Fig. 10 and not depicted). Thus, unlike Miro-1 in mammalian cells, Gem1p had no obvious role in these forms of yeast cell death.

Discussion

The mechanisms that allow mitochondria to receive or generate signals that modulate organelle shape and function are not well understood. Here, we show that cells lacking Gem1p have abnormal mitochondrial morphology and reduced respiratory function. Both GTPase domains and EF-hand motifs of Gem1p are required for its role in regulating mitochondrial dynamics. Gem1p is tail-anchored in the outer mitochondrial membrane, exposing these functional domains to the cytoplasm where they are available to interact with cell signaling pathways or other cellular structures. These findings suggest that Miro family members function in a novel pathway that integrates cell signaling with mitochondrial dynamics.

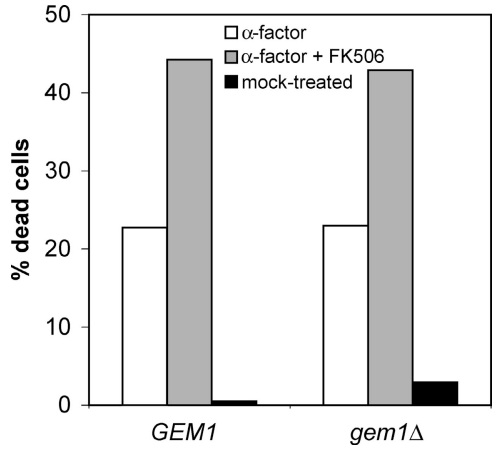

Figure 10. **Gem1p is not required for pheromone-induced cell death.** Cell death was induced by treating log phase cultures with 20 μM α-factor in the presence/absence of the calcineurin inhibitor FK506 (2 μg/ml). Dead cells were visualized after 10 h by methylene blue staining.

Table IV. **Conserved GTPase domains and EF-hand motifs of Gem1p are required for function**

gem1Δ strain containing pRS416 plus:	Percent tubular network	Percent collapsed	Percent mutant
No insert	0.9 ± 1.3	15.8 ± 3.4	83.3 ± 4.3
GEM1	59.9 ± 6.2	25.4 ± 5.7	14.6 ± 7.1
GTPase I domain mutations:			
gem1 (K18A)	3.1 ± 1.3	21.1 ± 3.5	75.8 ± 3.2
gem1 (S19N)	2.3 ± 0.9	18.6 ± 7.8	79.1 ± 7.4
gem1 (T33A)	57.8 ± 6.1	28.5 ± 4.7	13.7 ± 5.4
GTPase II domain mutations:			
gem1 (K461A)	13.1 ± 6.8	31.6 ± 13.8	55.3 ± 12.0
gem1 (S462N)	3.2 ± 2.6	16.7 ± 1.6	80.1 ± 2.4
gem1 (T480A)	13.9 ± 11.7	37.9 ± 10.3	48.3 ± 5.9
EF-hand motif mutations:			
gem1 (E225K)	28.7 ± 2.9	33.8 ± 2.4	37.5 ± 2.2
gem1 (E354K)	42.2 ± 3.5	30.7 ± 7.6	27.0 ± 10.4
gem1 (E225K, E354K)	14.3 ± 6.7	30.3 ± 4.9	55.3 ± 7.0

$n_{cells} > 300$.
Mitochondria were visualized by expressing mito-GFP.
Percent tubular network contains wild-type morphology shown in Fig. 3 A.
Percent collapsed contains aberrant morphology shown in Fig. 3 B.
Percent mutant category contains aberrant morphologies shown in Fig. 3 (C–E).

Members of the GTPase superfamily have evolved to regulate diverse processes by acting as binary molecular switches. Most GTPases contain a single nucleotide binding domain, raising the possibility that one of the Gem1p GTPase domains is an evolutionary relic and no longer functions. Our analysis demonstrates that both GTPase domains in a single Gem1p protein are required for activity. Specifically, mutations in the G1 motif (K to A or S to N) of either GTPase I or GTPase II abolish protein function. Thus, Gem1p function requires the nucleotide binding residues of both GTPase domains. Although changing the G2 conserved threonine to alanine dramatically alters Ras activity in vivo, similar mutations have no effect in GTPase I (Gem1p(T33A)), making it unlikely that this threonine residue mediates effector interactions required for maintenance of mitochondrial morphology. Moderate effects on Gem1p function were observed when a similar mutation was made in GTPase II (T480A; Table IV). Studies are in progress to characterize the nucleotide binding and hydrolysis activities of both Gem1p GTPase domains and identify potential Gem1p regulators.

EF-hand motifs have been shown to bind calcium, inducing a conformational change that alters protein activity (Yap et al., 1999; Lewit-Bentley and Rety, 2000; Ikura et al., 2002). Mutation of Gem1p EF-hand motifs demonstrated that conserved residues required for calcium coordination are important for Gem1p function (Table IV). Like other multiple EF-hand motif proteins (Janssens et al., 2003), mutation of both motifs produces a stronger phenotype than mutation of either alone. Whether calcium binding to Gem1p modulates protein–protein interactions, the GTPase cycle of either or both GTPase domains, or some other Gem1p function is not clear.

Several observations suggest that Gem1p is not an essential component of previously characterized pathways that control mitochondrial shape. Two processes, division and fusion, have been shown to control mitochondrial network morphology in fungi, invertebrates, and mammals. In tissue culture cells, overexpression of a hMiro-1 protein containing a putative activating mutation led to mitochondrial aggregation that could, in principle, result from decreased division and/or increased fusion (Fransson et al., 2003). Here, we demonstrate that mitochondrial fusion (Table II) and division (Table III) occur in *gem1*Δ cells, indicating that Gem1p is not a core component of the mitochondrial division or fusion machinery.

Studies have defined another yeast pathway that regulates mitochondrial shape. This pathway requires the function of four proteins: Mmm1p (Burgess et al., 1994), Mmm2p (Youngman et al., 2004), Mdm10p (Sogo and Yaffe, 1994), and Mdm12p (Berger et al., 1997). Mmm1p, Mdm10p, and Mdm12p have been shown to interact with each other, forming a complex on the outer mitochondrial membrane (Boldogh et al., 2003). Mmm2p is essential for formation of the Mmm1p-containing complex (Youngman et al., 2004), suggesting that all four proteins act in the same pathway. Additional studies indicate that this Mmm1p-containing complex is necessary for mtDNA replication and maintenance and spans both mitochondrial membranes (Burgess et al., 1994; Sogo and Yaffe, 1994; Berger et al., 1997; Aiken-Hobbs et al., 2001; Kondo-Okamoto et al., 2003; Meeusen and Nunnari, 2003).

When grown on dextrose medium, mutants lacking Mmm1p, Mdm10p, Mdm12p, or Mmm2p contain enlarged, spherical mitochondria somewhat similar to the globular organelles observed in 54% of dextrose-grown *gem1*Δ cells (Fig. 3). Although these findings suggest that Gem1p may be required for the function of these four proteins, several lines of evidence argue against this possibility. First, large spherical mitochondria occur in *mmm1*Δ, *mmm2*Δ, *mdm10*Δ, and *mdm12-1* cells grown in a variety of media (Burgess et al., 1994; Sogo and Yaffe, 1994; Berger et al., 1997; Youngman et al., 2004). In contrast, mitochondria are not spherical or globular in most *gem1*Δ cells grown in synthetic glycerol medium. Instead, *gem1*Δ cells contain short, tubular mitochondria (unpublished data). Second, Mmm1p-GFP localizes properly in cells lacking Gem1p (Fig. 9 D). Because Mmm2p, Mdm10p, and Mdm12p are required for proper Mmm1p lo-

calization on mitochondria (Boldogh et al., 2003; Kondo-Okamoto et al., 2003; Youngman et al., 2004), it seems likely that all four proteins function normally in *gem1*Δ cells. Third, steady-state levels of Mmm1p and Mmm2p are indistinguishable between *GEM1* and *gem1*Δ strains (unpublished data). Fourth, when grown on dextrose medium, most *mmm1*Δ, *mmm2*Δ, *mdm10*Δ, and *mdm12*Δ strains exhibit significant mtDNA instability and lose mtDNA (Berger et al., 1997; Youngman et al., 2004). In contrast, DAPI staining of cells grown for at least 35 generations in dextrose-containing media revealed that 43% of *gem1*Δ cells maintain visible mtDNA (Fig. S1). Fifth, although deletion of *MMM1* causes abnormal inner mitochondrial membrane structure (Aiken-Hobbs et al., 2001), *gem1* null mutants grown in glycerol- or dextrose-containing media maintain inner membrane cristae (Fig. 4 and not depicted). Together, these observations suggest that Gem1p is not essential for the function of Mmm1p-containing complexes.

Mitochondrial attachment to actin filaments is also required for normal mitochondrial morphology and transport of the organelle from mother to bud during cell division (Drubin et al., 1993; Lazzarino et al., 1994; Hermann et al., 1997; Boldogh et al., 1998, 2003). However, *gem1*Δ cells do not exhibit defects in mitochondrial inheritance (Fig. 5), suggesting that mitochondrial–actin interactions remain intact in this mutant. In addition, Gem1p does not appear to regulate actin organization as actin cables and patches are normal in *gem1*Δ mutants.

Although Fransson et al. (2003) suggested that a mutant Miro-1 protein had a pro-apoptotic function in tissue culture cells, whether Miro-1 was required to induce cell death was not tested. Here, we showed that Gem1p is not required for pheromone induced cell death in yeast. Although it is formally possible that Gem1p participates in other forms of yeast cell death (Madeo et al., 2002; Wysocki and Kron, 2004), our combined results support a primary role for Gem1p in mitochondrial morphology maintenance.

Gem1p does not appear to be essential for any of the known pathways controlling mitochondrial morphology in yeast. The localization and topology of Gem1p suggest that it may sense cytoplasmic signals (e.g., cytosolic calcium, other signaling molecules) and directly or indirectly alter mitochondrial morphology. Several observations support the notion that Gem1p is a regulatory molecule. First, a large portion of Gem1p is devoted to domains that act as molecular switches in other proteins, and these domains are required for Gem1p function. Second, unlike mutants which disrupt division, fusion, or the Mmm1p morphology pathway, *gem1*Δ cells exhibit pleiotropic mitochondrial morphologies (Fig. 3). Third, changing the cellular environment by altering strain background or carbon source alters the severity of the *gem1*Δ mitochondrial phenotype. One attractive hypothesis currently being tested is that Gem1p regulates mitochondrial morphology pathways in response to changes in cytosolic calcium levels. Identification of protein binding partners for Gem1p is in progress and will likely reveal the pathways in which Gem1p acts.

Materials and methods

Strains and plasmid constructions

Yeast strains were constructed in the W303 background. Standard methods were used to manipulate yeast (Sherman et al., 1986; Guthrie and Fink, 1991) and bacterial (Maniatis et al., 1982) strains. All mutations, disruptions, and constructs were confirmed by PCR, DNA sequencing, and, where appropriate, Western blotting.

A complete disruption of YAL048C (*GEM1*) coding region was accomplished by homologous recombination using a *HIS3* cassette (Rothstein, 1991) generating strain JSY6592 (MAT *ade2-1 leu2-3 his3-11,15 trp1-1 ura3-1 can1-100 gem1::HIS3*). A backcross of this strain to W303 wild type generated the wild-type JSY7000 (MAT *ade2-1 leu2-3 his3-11,15 trp1-1 ura3-1 can1-100*) and *gem1*Δ JSY7002 (MAT α *ade2-1 leu2-3 his3-11,15 trp1-1 ura3-1 can1-100 gem1::HIS3*) strains. Double mutants of *gem1* and other genes were generated by mating, sporulation, and dissection. To generate JSY7234 (MAT **a** *ade2-1 leu2-3 his3-11 trp1-1 ura3-1 can1-100 gem1::HIS3 dnm1::HIS3*) and JSY7236 (MAT α *ade2-1 leu2-3 his3-11 trp1-1 ura3-1 can1-100 gem1::HIS3 dnm1::HIS3*), JSY6592 was crossed to JSY5138 (MAT **a** *ade2-1 leu2-3 his3-11 trp1-1 ura3-1 can1-100 dnm1::HIS3*). To make JSY7266 (MAT α *ade2-1 leu2-3 his3-11,15 trp1-1 ura3-1 can1-100 gem1::HIS3 fzo1::TRP1*) and JSY7268 (MAT **a** *ade2-1 leu2-3 his3-11, 15 trp1-1 ura3-1 can1-100 GEM1 fzo1::TRP1*), JSY7001 (MAT α *ade2-1 leu2-3 his3-11,15 trp1-1 ura3-1 can1-100 gem1::HIS3*) was mated to JSY6997(MAT **a** *ade2-1 leu2-3 his3-11,15 trp1-1 ura3-1 can1-100 fzo1::TRP1*).

pRS416-*GEM1* contains the complete *GEM1* coding sequence flanked by 1507 bp 5′ to the ATG and 300 bp 3′ of the stop codon. A SpeI site inserted at the 5′ end of the coding region converted the NH_2-terminal amino acid sequence from MTK to MTSTK. These two additional amino acids are functionally silent; this construct and constructs lacking these extra amino acids rescue *gem1*Δ morphology defects to the same extent (Table I). A translationally silent BspEI site was introduced at L619 by site-directed mutagenesis (Stratagene) to generate pRS416-*GEM1*. For pYX142-GFP, a PCR fragment encoding GFP and flanked by HindIII and EcoRI was cloned into pYX142. GFP fusions in this vector are driven by the constitutively active TPI promoter. For pYX142-GFP-*GEM1* and pYX142-GFP-*GEM1*(aa618-662), a *GEM1* PCR fragment flanked by HindIII and SacI sites was cloned into pYX142-GFP.

Plasmids for analysis of specific domain mutations were generated by site-directed mutagenesis (Stratagene) of pRS416-*GEM1* and included pRS416-*GEM1*(K18A), pRS416-*GEM1*(S19N), pRS416-*GEM1*(K461A), pRS416-*GEM1*(S462N), pRS416-*GEM1*(E225K), and pRS416-*GEM1*(T480A). pRS416-*GEM1*(T33A) and pRS416-*GEM1*(E354K) were generated using three-way homologous recombination in yeast (Kitagawa and Abdulle, 2002). To generate the plasmid containing both EF-hand motif mutations, a SnaBI and SacI fragment derived from pRS416-*GEM1*(E225K) was ligated into pRS416-*GEM1*(E354K) digested with the same enzymes. Expression of mutant proteins that abrogate function was verified by GFP tagging and in vivo localization.

For serial dilutions, strains JSY7000 *GEM1* or JSY7002 *gem1*Δ containing the indicated plasmid were grown in SDextrose dropout medium to early log phase (OD_{600} 0.5–1.0), pelleted, and resuspended to OD_{600} 0.5. Aliquots of 1:5 serial dilutions were spotted onto SDextrose or SGlycerol medium lacking the appropriate amino acids and grown for 3 d at the indicated temperatures.

Analysis of mitochondrial morphology, mitochondrial fusion, mtDNA maintenance, and actin cytoskeleton

Mitochondrial morphology was scored at 30°C in wild-type and mutant cells expressing a matrix targeted form of mito-GFP (pYX142-mtGFP+) or mito-RFP (p414GPD-mtRFPff) grown to mid-log phase (OD_{600} 0.5–1.0) in dextrose-containing medium, unless otherwise indicated. In some cases, mitochondria were labeled with MitoFluor red 589 (Molecular Probes, Inc.). Phenotypes were quantified in at least 100 cells in three or more independent experiments. Data reported are the average and SD of all experiments with *n* representing the total number of cells observed. Mitochondrial fusion during mating was performed as described previously (Mozdy et al., 2000). Large-budded zygotes were scored 2.5–4 h after mating on YPD. DAPI staining was used to visualize mtDNA nucleoids (Williamson and Fennell, 1979). Alexa-phalloidin staining of yeast actin was performed as described previously (Singer et al., 2000).

Microscopy and image acquisition

Digital fluorescence and DIC microscopic images of cells grown in synthetic dextrose were acquired using an Axioplan 2 deconvolution micro-

scope (Carl Zeiss MicroImaging, Inc.). For Fig. 3, Z-stacks of 0.3-μm slices were obtained using a 500-ms exposure (1 s for Fig. 3 E) and deconvolved using an inverse regularized filter algorithm. Images were assembled into figures using Adobe Photoshop 10.0 using only linear adjustments of contrast and brightness. TEM was performed essentially as described previously (Rieder et al., 1996) using cells grown in YPGlycerol.

Subcellular and submitochondrial localization of GFP-Gem1p

JSY7000 cells containing pYX142-GFP-*GEM1* were grown in lactate medium to log phase (OD_{600} 0.6–1.0), spheroplasted, lysed, and subjected to differential sedimentation to generate an enriched mitochondrial fraction as described previously (Kondo-Okamoto et al., 2003). WCE, PMS, and MITO fractions were separated by SDS-PAGE and analyzed by Western blotting with antibodies specific for Porin (Molecular Probes, 1:8,000), 3-PGK (Molecular Probes, 1:1,000), and GFP (Covance, Inc., 1:500). HRP-conjugated secondary antibody (goat α mouse; Sigma-Aldrich, 1:10,000; goat α rabbit; Jackson ImmunoResearch Laboratories, 1:10,000) and ECL detection were used to visualize bands. MITO (30 μg protein) were loaded at 10-fold more (cell equivalents) than WCE and PMS.

Mitochondria (200 μg protein) were analyzed by protease protection as described previously (Kondo-Okamoto et al., 2003). Samples were subjected to PK treatment, osmotic shock and PK treatment, detergent solubilization and PK treatment, or a mock treatment. Samples were denatured and analyzed by SDS-PAGE and Western blotting (one quarter of total reaction per lane). To perform carbonate extraction, mitochondria (200 μg) were treated with 0.1 M Na_2CO_3, pH 11.5, and the sample was spun at 150,000 *g* for 10 min. The membrane pellet and TCA-precipitated supernatant were solubilized and analyzed by SDS-PAGE and Western blotting. pAbs used were as follows: αmtHsp70 (1:8,000, a gift from W. Neupert, University of Munich, Munich, Germany), αCyb2p (1:10,000, a gift from T. Endo, Nagoya University, Nagoya, Japan), αTim50p (1:10,000, a gift from T. Endo), αFzo1p (1:5,000), αMge1p (1:5,000, a gift from T. Endo), and αTim44p (1:5,000, a gift from K. Hell, University of Munich, Munich, Germany).

Pheromone-induced cell death

GEM1 and *gem1*Δ cells were grown to early log phase in YPD and diluted to OD < 0.02. Cells were treated with α-factor (20 μM; US Biologicals), α-factor and FK506 (2 μg/ml; A.G. Scientific, Inc.), or mock-treated with DMSO only. After 10 h, cells were stained with methylene blue (100 μg/ml) and observed using bright field microscopy. Results shown are the averages of two independent experiments in which $n = 200$ for each treatment.

Online supplemental material

mtDNA maintenance during growth in dextrose-containing medium is depicted in Fig. S1. Online supplemental material is available at http://www.jcb.org/cgi/content/full/jcb.200405100/DC1.

We greatly appreciate discussions with all members of the Shaw lab. We thank W. Neupert, K. Hell, M. Yaffe, R. Jensen, and T. Endo for their gifts of antibodies, B. Glick for a plasmid encoding FastFold RFP, and W. Prinz for a plasmid encoding Sec63-GFP. We thank Nousheen Alasti for constructing pRS415-*MET25*-GFP-*MDV1*.

This work was funded by a grant from the National Institutes of Health awarded to J.M. Shaw (GM53466), a grant from the United Mitochondrial Disease Foundation awarded to K. Okamoto, and a National Science Foundation Graduate Research Fellowship awarded to R.L. Frederick. The Utah Health Sciences DNA/Peptide and Sequencing Facilities are supported by a National Cancer Institute grant (5-P30CA42014).

Submitted: 17 May 2004
Accepted: 31 August 2004

References

Aiken-Hobbs, A.E., M. Srinivasan, J.M. McCaffery, and R.E. Jensen. 2001. Mmm1p, a mitochondrial outer membrane protein, is connected to mitochondrial DNA (mtDNA) nucleoids and required for mtDNA stability. *J. Cell Biol.* 152:401–410.

Berger, K.H., L.F. Sogo, and M.P. Yaffe. 1997. Mdm12p, a component required for mitochondrial inheritance that is conserved between budding and fission yeast. *J. Cell Biol.* 136:545–553.

Bleazard, W., J.M. McCaffery, E.J. King, S. Bale, A. Mozdy, Q. Tieu, J. Nunnari, and J.M. Shaw. 1999. The dynamin-related GTPase Dnm1 regulates mitochondrial fission in yeast. *Nat. Cell Biol.* 1:298–304.

Boldogh, I., N. Vojtov, S. Karmon, and L.A. Pon. 1998. Interaction between mitochondria and the actin cytoskeleton in budding yeast requires two integral mitochondrial outer membrane proteins, Mmm1p and Mdm10p. *J. Cell Biol.* 141:1371–1381.

Boldogh, I.R., D.W. Nowakowski, H.C. Yang, H. Chung, S. Karmon, P. Royes, and L.A. Pon. 2003. A protein complex containing Mdm10p, Mdm12p, and Mmm1p links mitochondrial membranes and DNA to the cytoskeleton-based segregation machinery. *Mol. Biol. Cell.* 14:4618–4627.

Borgese, N., S. Colombo, and E. Pedrazzini. 2003. The tale of tail-anchored proteins: coming from the cytosol and looking for a membrane. *J. Cell Biol.* 161:1013–1019.

Bourne, H.R., D.A. Sanders, and F. McCormick. 1991. The GTPase superfamily: conserved structure and molecular mechanism. *Nature.* 349:117–127.

Brini, M., and E. Carafoli. 2000. Calcium signalling: a historical account, recent developments and future perspectives. *Cell. Mol. Life Sci.* 57:354–370.

Burgess, S.M., M. Delannoy, and R.E. Jensen. 1994. MMM1 encodes a mitochondrial outer membrane protein essential for establishing and maintaining the structure of yeast mitochondria. *J. Cell Biol.* 126:1375–1391.

Cales, C., J.F. Hancock, C.J. Marshall, and A. Hall. 1988. The cytoplasmic protein GAP is implicated as the target for regulation by the ras gene product. *Nature.* 332:548–551.

Cerveny, K.L., J.M. McCaffery, and R.E. Jensen. 2001. Division of mitochondria requires a novel DNM1-interacting protein, Net2p. *Mol. Biol. Cell.* 12:309–321.

Chen, H., and D.C. Chan. 2004. Mitochondrial dynamics in mammals. *Curr. Top. Dev. Biol.* 59:119–144.

Cyert, M.S., and J. Thorner. 1992. Regulatory subunit (CNB1 gene product) of yeast Ca^{2+}/calmodulin-dependent phosphoprotein phosphatases is required for adaptation to pheromone. *Mol. Cell. Biol.* 12:3460–3469.

Cyert, M.S., R. Kunisawa, D. Kaim, and J. Thorner. 1991. Yeast has homologs (CNA1 and CNA2 gene products) of mammalian calcineurin, a calmodulin-regulated phosphoprotein phosphatase. *Proc. Natl. Acad. Sci. USA.* 88:7376–7380.

Drubin, D.G., H.D. Jones, and K.F. Wertman. 1993. Actin structure and function: roles in mitochondrial organization and morphogenesis in budding yeast and identification of the phalloidin-binding site. *Mol. Biol. Cell.* 4:1277–1294.

Feig, L.A., and G.M. Cooper. 1988. Inhibition of NIH 3T3 cell proliferation by a mutant ras protein with preferential affinity for GDP. *Mol. Cell. Biol.* 8:3235–3243.

Fekkes, P., K.A. Shepard, and M.P. Yaffe. 2000. Gag3p, an outer membrane protein required for fission of mitochondrial tubules. *J. Cell Biol.* 151: 333–340.

Feng, B., and P.M. Stemmer. 2001. Ca^{2+} binding site 2 in calcineurin-B modulates calmodulin-dependent calcineurin phosphatase activity. *Biochemistry.* 40:8808–8814.

Foor, F., S.A. Parent, N. Morin, A.M. Dahl, N. Ramadan, G. Chrebet, K.A. Bostian, and J.B. Nielsen. 1992. Calcineurin mediates inhibition by FK506 and cyclosporin of recovery from alpha-factor arrest in yeast. *Nature.* 360:682–684.

Frank, S., B. Gaume, E.S. Bergmann-Leitner, W.W. Leitner, E.G. Robert, F. Catez, C.L. Smith, and R.J. Youle. 2001. The role of dynamin-related protein 1, a mediator of mitochondrial fission, in apoptosis. *Dev. Cell.* 1:515–525.

Fransson, A., A. Ruusala, and P. Aspenstrom. 2003. Atypical Rho GTPases have roles in mitochondrial homeostasis and apoptosis. *J. Biol. Chem.* 278:6495–6502.

Guthrie, C., and G. Fink. 1991. Yeast genetics and molecular biology. *In* Methods in Enzymology. Vol. 194. J.N. Abelson and M.I. Simon, editors. Academic Press, Inc., San Diego, CA. 1–933.

Habib, S.J., A. Vasiljev, W. Neupert, and D. Rapaport. 2003. Multiple functions of tail-anchor domains of mitochondrial outer membrane proteins. *FEBS Lett.* 555:511–515.

Hermann, G.J., and J.M. Shaw. 1998. Mitochondrial dynamics in yeast. *Annu. Rev. Cell Dev. Biol.* 14:265–303.

Hermann, G.J., E.J. King, and J.M. Shaw. 1997. The yeast gene, MDM20, is necessary for mitochondrial inheritance and organization of the actin cytoskeleton. *J. Cell Biol.* 137:141–153.

Hermann, G.J., J.W. Thatcher, J.P. Mills, K.G. Hales, M.T. Fuller, J. Nunnari, and J.M. Shaw. 1998. Mitochondrial fusion in yeast requires the transmembrane GTPase Fzo1p. *J. Cell Biol.* 143:359–373.

Hill, K.L., N.L. Catlett, and L.S. Weisman. 1996. Actin and myosin function in directed vacuole movement during cell division in *Saccharomyces cerevisiae*. *J. Cell Biol.* 135:1535–1549.

Horie, C., H. Suzuki, M. Sakaguchi, and K. Mihara. 2003. Targeting and assembly of mitochondrial tail-anchored protein Tom5 to the TOM complex

depend on a signal distinct from that of tail-anchored proteins dispersed in the membrane. *J. Biol. Chem.* 278:41462–41471.

Iida, H., Y. Yagawa, and Y. Anraku. 1990. Essential role for induced Ca^{2+} influx followed by $[Ca^{2+}]_i$ rise in maintaining viability of yeast cells late in the mating pheromone response pathway. A study of $[Ca^{2+}]_i$ in single *Saccharomyces cerevisiae* cells with imaging of fura-2. *J. Biol. Chem.* 265:13391–13399.

Ikura, M. 1996. Calcium binding and conformational response in EF-hand proteins. *Trends Biochem. Sci.* 21:14–17.

Ikura, M., M. Osawa, and J.B. Ames. 2002. The role of calcium-binding proteins in the control of transcription: structure to function. *Bioessays.* 24: 625–636.

Jacobson, J., and M.R. Duchen. 2004. Interplay between mitochondria and cellular calcium signalling. *Mol. Cell. Biochem.* 256-257:209–218.

Janssens, V., J. Jordens, I. Stevens, C. Van Hoof, E. Martens, H. De Smedt, Y. Engelborghs, E. Waelkens, and J. Goris. 2003. Identification and functional analysis of two Ca^{2+}-binding EF-hand motifs in the B"/PR72 subunit of protein phosphatase 2A. *J. Biol. Chem.* 278:10697–10706.

Jensen, R.E., A.E. Hobbs, K.L. Cerveny, and H. Sesaki. 2000. Yeast mitochondrial dynamics: fusion, division, segregation, and shape. *Microsc. Res. Tech.* 51:573–583.

Kitagawa, K., and R. Abdulle. 2002. In vivo site-directed mutagenesis of yeast plasmids using a three-fragment homologous recombination system. *Biotechniques*. 33:288, 290, 292 passim.

Kondo-Okamoto, N., J.M. Shaw, and K. Okamoto. 2003. Mmm1p spans both the outer and inner mitochondrial membranes and contains distinct domains for targeting and foci formation. *J. Biol. Chem.* 278:48997–49005.

Koning, A.J., P.Y. Lum, J.M. Williams, and R. Wright. 1993. DiOC6 staining reveals organelle structure and dynamics in living yeast cells. *Cell Motil. Cytoskeleton.* 25:111–128.

Lazzarino, D.A., I. Boldogh, M.G. Smith, J. Rosand, and L.A. Pon. 1994. Yeast mitochondria contain ATP-sensitive, reversible actin-binding activity. *Mol. Biol. Cell.* 5:807–818.

Lewit-Bentley, A., and S. Rety. 2000. EF-hand calcium-binding proteins. *Curr. Opin. Struct. Biol.* 10:637–643.

Madeo, F., S. Engelhardt, E. Herker, N. Lehmann, C. Maldener, A. Proksch, S. Wissing, and K.U. Frohlich. 2002. Apoptosis in yeast: a new model system with applications in cell biology and medicine. *Curr. Genet.* 41:208–216.

Maniatis, T., E.F. Fritsch, and J. Sambrook. 1982. Molecular Cloning: A Laboratory Manual. Cold Spring Harbor Laboratory, Cold Spring Harbor, NY. 545 pp.

Meeusen, S., and J. Nunnari. 2003. Evidence for a two membrane-spanning autonomous mitochondrial DNA replisome. *J. Cell Biol.* 163:503–510.

Mokranjac, D., M. Sichting, W. Neupert, and K. Hell. 2003. Tim14, a novel key component of the import motor of the TIM23 protein translocase of mitochondria. *EMBO J.* 22:4945–4956.

Moser, M.J., J.R. Geiser, and T.N. Davis. 1996. Ca^{2+}-calmodulin promotes survival of pheromone-induced growth arrest by activation of calcineurin and Ca^{2+}-calmodulin-dependent protein kinase. *Mol. Cell. Biol.* 16: 4824–4831.

Mozdy, A.D., and J.M. Shaw. 2003. A fuzzy mitochondrial fusion apparatus comes into focus. *Nat. Rev. Mol. Cell Biol.* 4:468–478.

Mozdy, A.D., J.M. McCaffery, and J.M. Shaw. 2000. Dnm1p GTPase-mediated mitochondrial fission is a multi-step process requiring the novel integral membrane component Fis1p. *J. Cell Biol.* 151:367–380.

Muller, E.M., E.G. Locke, and K.W. Cunningham. 2001. Differential regulation of two $Ca^{(2+)}$ influx systems by pheromone signaling in *Saccharomyces cerevisiae*. *Genetics.* 159:1527–1538.

Nakayama, S., and R.H. Kretsinger. 1994. Evolution of the EF-hand family of proteins. *Annu. Rev. Biophys. Biomol. Struct.* 23:473–507.

Nunnari, J., W.F. Marshall, A. Straight, A. Murray, J.W. Sedat, and P. Walter. 1997. Mitochondrial transmission during mating in *Saccharomyces cerevisiae* is determined by mitochondrial fusion and fission and the intramitochondrial segregation of mitochondrial DNA. *Mol. Biol. Cell.* 8:1233–1242.

Osteryoung, K.W., and J. Nunnari. 2003. The division of endosymbiotic organelles. *Science.* 302:1698–1704.

Otsuga, D., B.R. Keegan, E. Brisch, J.W. Thatcher, G.J. Hermann, W. Bleazard, and J.M. Shaw. 1998. The dynamin-related GTPase, Dnm1p, controls mitochondrial morphology in yeast. *J. Cell Biol.* 143:333–349.

Prinz, W.A., L. Grzyb, M. Veenhuis, J.A. Kahana, P.A. Silver, and T.A. Rapoport. 2000. Mutants affecting the structure of the cortical endoplasmic reticulum in *Saccharomyces cerevisiae*. *J. Cell Biol.* 150:461–474.

Rieder, S.E., L.M. Banta, K. Kohrer, J.M. McCaffery, and S.D. Emr. 1996. Multilamellar endosome-like compartment accumulates in the yeast vps28 vacuolar protein sorting mutant. *Mol. Biol. Cell.* 7:985–999.

Rizzuto, R., P. Pinton, D. Ferrari, M. Chami, G. Szabadkai, P.J. Magalhaes, F. Di Virgilio, and T. Pozzan. 2003. Calcium and apoptosis: facts and hypotheses. *Oncogene.* 22:8619–8627.

Rothstein, R. 1991. Targeting, disruption, replacement, and allele rescue: integrative DNA transformation in yeast. *Methods Enzymol.* 194:281–301.

Sayer, R.J. 2002. Intracellular Ca^{2+} handling. *Adv. Exp. Med. Biol.* 513:183–196.

Scott, S.V., A. Cassidy-Stone, S.L. Meeusen, and J. Nunnari. 2003. Staying in aerobic shape: how the structural integrity of mitochondria and mitochondrial DNA is maintained. *Curr. Opin. Cell Biol.* 15:482–488.

Sesaki, H., and R.E. Jensen. 1999. Division versus fusion: Dnm1p and Fzo1p antagonistically regulate mitochondrial shape. *J. Cell Biol.* 147:699–706.

Sesaki, H., and R.E. Jensen. 2001. UGO1 encodes an outer membrane protein required for mitochondrial fusion. *J. Cell Biol.* 152:1123–1134.

Severin, F.F., and A.A. Hyman. 2002. Pheromone induces programmed cell death in *S. cerevisiae*. *Curr. Biol.* 12:R233–R235.

Shaw, J.M., and J. Nunnari. 2002. Mitochondrial dynamics and division in budding yeast. *Trends Cell Biol.* 12:178–184.

Sherman, F., G.R. Fink, and J.B. Hicks. 1986. Methods in Yeast Genetics. Cold Spring Harbor Laboratory Press, Cold Spring Harbor, NY. 186 pp.

Sigal, I.S., J.B. Gibbs, J.S. D'Alonzo, G.L. Temeles, B.S. Wolanski, S.H. Socher, and E.M. Scolnick. 1986. Mutant ras-encoded proteins with altered nucleotide binding exert dominant biological effects. *Proc. Natl. Acad. Sci. USA.* 83:952–956.

Singer, J.M., G.J. Hermann, and J.M. Shaw. 2000. Suppressors of mdm20 in yeast identify new alleles of ACT1 and TPM1 predicted to enhance actin-tropomyosin interactions. *Genetics.* 156:523–534.

Sogo, L.F., and M.P. Yaffe. 1994. Regulation of mitochondrial morphology and inheritance by Mdm10p, a protein of the mitochondrial outer membrane. *J. Cell Biol.* 126:1361–1373.

Stevens, B. 1981. Mitochondrial structure. *In* The Molecular Biology of the Yeast *Saccharomyces*. J.M. Strathern, E.W. Jones, and J.R. Broach, editors. Cold Spring Harbor Laboratory Press, Cold Spring Harbor, NY. 471–504.

Tieu, Q., and J. Nunnari. 2000. Mdv1p is a WD repeat protein that interacts with the dynamin-related GTPase, Dnm1p, to trigger mitochondrial division. *J. Cell Biol.* 151:353–366.

Truscott, K.N., W. Voos, A.E. Frazier, M. Lind, Y. Li, A. Geissler, J. Dudek, H. Muller, A. Sickmann, H.E. Meyer, et al. 2003. A J-protein is an essential subunit of the presequence translocase-associated protein import motor of mitochondria. *J. Cell Biol.* 163:707–713.

Wattenberg, B., and T. Lithgow. 2001. Targeting of C-terminal (tail)-anchored proteins: understanding how cytoplasmic activities are anchored to intracellular membranes. *Traffic.* 2:66–71.

Wennerberg, K., and C.J. Der. 2004. Rho-family GTPases: it's not only Rac and Rho (and I like it). *J. Cell Sci.* 117:1301–1312.

Westermann, B. 2002. Merging mitochondria matters: cellular role and molecular machinery of mitochondrial fusion. *EMBO Rep.* 3:527–531.

Westermann, B. 2003. Mitochondrial membrane fusion. *Biochim. Biophys. Acta.* 1641:195–202.

Williamson, D.H., and D.J. Fennell. 1979. Visualization of yeast mitochondrial DNA with the fluorescent stain "DAPI". *Methods Enzymol.* 56:728–733.

Withee, J.L., J. Mulholland, R. Jeng, and M.S. Cyert. 1997. An essential role of the yeast pheromone-induced Ca^{2+} signal is to activate calcineurin. *Mol. Biol. Cell.* 8:263–277.

Wolff, A.M., J.G. Petersen, T. Nilsson-Tillgren, and N. Din. 1999. The open reading frame YAL048c affects the secretion of proteinase A in *S. cerevisiae*. *Yeast.* 15:427–434.

Wysocki, R., and S.J. Kron. 2004. Yeast cell death during DNA damage arrest is independent of caspase or reactive oxygen species. *J. Cell Biol.* 166: 311–316.

Yaffe, M.P. 1999. The machinery of mitochondrial inheritance and behavior. *Science.* 283:1493–1497.

Yap, K.L., J.B. Ames, M.B. Swindells, and M. Ikura. 1999. Diversity of conformational states and changes within the EF-hand protein superfamily. *Proteins.* 37:499–507.

Yoon, Y., and M.A. McNiven. 2001. Mitochondrial division: new partners in membrane pinching. *Curr. Biol.* 11:R67–R70.

Youngman, M.J., A.E. Hobbs, S.M. Burgess, M. Srinivasan, and R.E. Jensen. 2004. Mmm2p, a mitochondrial outer membrane protein required for yeast mitochondrial shape and maintenance of mtDNA nucleoids. *J. Cell Biol.* 164:677–688.